Evaluation of a Commercial Mammography Image-Enhancement System

Richard H. Behrman, Robert G. Zamenhof, and Katherine M. Blazo

A commercial mammography image-enhancement system manufactured by Damon Corporation (Needham, MA) is evaluated. Using a dedicated computer, the system implements a real-time video local adaptive image processing algorithm based on the Wallis equation. Radiographs of a mammographic QA phantom (Nuclear Associates Model 76-001-4) containing five groups of simulated breast microcalcifications ranging in diameter from 0.12 to 0.35 mm were viewed by four investigators under three viewing conditions: on a light box with the unaided eye, on the image enhancer in magnified "bypass" (unenhanced) mode, and on the enhancer using all features for optimum enhancement. A mammogram was then overlaid on the radiographs, and the composite images were viewed under the same three conditions. Using the enhancer, as compared to using a light box alone, average increases of 1.4 and 1.1 microcalcifications per radiograph were observed for the phantom and phantom-with-mammogram radiographs, respectively. High-contrast resolution and spatial distortion were also measured.

A SIGNIFICANT EARLY indicator of malignant breast disease is the presence of microcalcifications in the breast. These structures, which have a high calcium content, show up as small radiopaque specks on mammograms because of the high x-ray attenuation of calcium relative to soft tissue. With state-of-the-art equipment, microcalcifications smaller than 0.2 mm in diameter can be detected. Great efforts have been made to optimize detection of these objects with dedicated mammographic equipment using low kilovoltages to enhance image contrast, high resolution film/screen systems with small focal spot techniques to maximize image sharpness, and new developments in xeroradiography.[1,2] More recently, radiographic image-enhancement processing systems have been developed to assist radiologists in reading films.[3,4,5,6] This report describes and evaluates a particular commercial image-enhancement system manufactured by Damon Corporation (Needham, MA) that is designed primarily for use in mammography. A unit has been on loan to the Departments of Radiology and Radiation Oncology at Tufts–New England Medical Center for such an evaluation.

DESCRIPTION OF THE IMAGE ENHANCER

The Damon image enhancer (Fig 1) consists of a light box over which a mammogram (or any radiographic film) can be placed. A video camera located above the film transmits an electronic 525-line image of the film to a computer, which digitizes and processes the image. The final processed image is displayed on a television monitor. The image processing takes place at a screen refresh rate of 30 times per second, so that the film can be moved over the light box, allowing different regions of the film to be enhanced and displayed on the monitor in "real time." Through use of a joy stick, parameters affecting local contrast and local background density can be continuously adjusted as the image is displayed (Fig 2). Additional controls include IMAGE REVERSAL, EDGE ENHANCEMENT, CIRCULAR REGION OF INTEREST, and SPLIT-SCREEN buttons. Image magnification can be continuously increased to a maximum of 4.3:1 via a thumb-wheel control.

The heart of the enhancer is a dedicated computer that implements a real-time local adaptive video processing algorithm based on the Wallis equation.[7,8,9] Image enhancement on most digital radiographic, magnetic resonance imaging, or computed tomography (CT) equipment is limited to global enhancement; that is, all the pixels in an image are changed according to a global criterion. For example, on a CT monitor or a digital radiographic display, contrast and background are changed by adjusting the window size and level settings, respectively. These controls change the value of all the pixels on the screen according to a single universal rule. Similarly, in fluoroscopy, the brightness and contrast controls for the television monitor are also global. In local

From the Medical Physics Division, Department of Radiation Oncology, Tufts–New England Medical Center, Boston, MA.

Address reprint requests to Richard H. Behrman, PhD, Medical Physics Division, Box 246, Tufts–New England Medical Center, 750 Washington St, Boston MA, 02111.

0897-1889/89/0203-0005$03.00/0

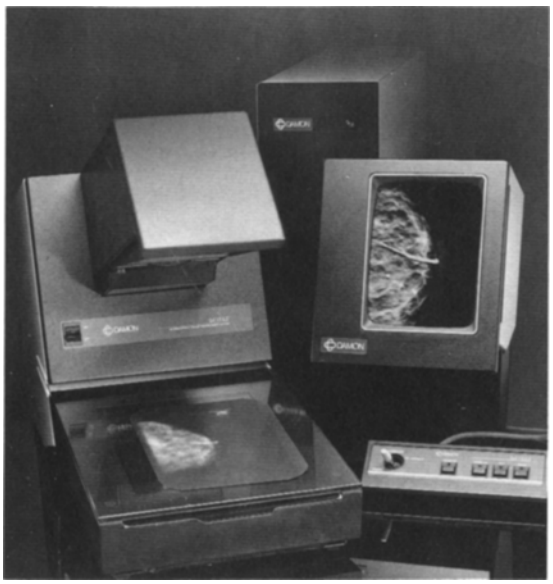

Fig 1. The Damon Mammographic Image Enhancer.

adaptive processing, each pixel in a digitized image is surrounded by a region of selectable size. The final (processed) value of this pixel depends on the local contrast and background level in this region. This dependency on local parameters is what makes an algorithm locally adaptive.

The Wallis equation can be written as

$$z_i = \frac{(x_i - \bar{x})}{\left(\frac{\sigma_x}{\sigma_D} + \frac{1}{A}\right)} + \bar{x} + \alpha(x_D - \bar{x}) \qquad \text{(Equation 1)}$$

where x_i is the original pixel value (intensity) assigned to the ith pixel by the analogue to digital converter, and z_i is the final processed (or enhanced) pixel value displayed on the television monitor. $\bar{x}$ is the average pixel value (local background intensity) within a predefined aperture or local region surrounding x_i, and σ_x is the standard deviation of the pixel values in this same region. Because the standard deviation is a measure of the spread in pixel values, it corresponds to contrast.

The effect of the Wallis equation is to produce an average contrast, σ_D, that is approximately the same for all regions across the screen, and an average local background intensity, $\bar{z}$, given by

$$\bar{z} = \bar{x} + \alpha(x_D - \bar{x}) \qquad \text{(Equation 2)}$$

which varies from region to region. x_D is some "desired" global background intensity and $\bar{x}$, the local background intensity, as defined above. The parameter α is a local background subtract control such that $\bar{z} = x_D$ for $\alpha = 1$, and $\bar{z} = \bar{x}$ for $\alpha = 0$. A in Equation 1 serves to keep z_i within finite limits for regions where the local contrast is very small ($\sigma_x \cong 0$).

By use of a joystick, the Damon system uses an approximation of Equation 1, whereby only σ_D (contrast) and α (background subtract) are set by the user. A bypass position also exists so that the original unenhanced image ($z_i = x_i$) appears on the monitor. A and x_D, as well as local region size, are fixed internally by the manufacturer. The pixel matrix is 750 × 480 and is 11 bits deep (2048 gray levels.)

HIGH-CONTRAST RESOLUTION

The high-contrast resolution of the Damon image enhancer was measured by using high-contrast contact radiographs of a fluoroscopic test pattern (line pairs [lp] ranging from 0.63 lp/mm to 4.82 lp/mm), and a radiographic test pattern (ranging from 2 lp/mm to 10 lp/mm). The test pattern radiographs were oriented at approximately 45° from the horizontal. Radiographs were used in place of the test patterns themselves to eliminate light reflection between the lead bars of the test patterns when they were placed on the light box of the enhancer. Resolution as a function of magnification is shown in Fig 3, and varies between 2 lp/mm at 1:1 magnification to 7.1 lp/mm at 4.3:1 magnification (maximum).

IMAGE DISTORTION

Spatial distortion was measured by placing a transparent ruler on the light box (oriented first in the horizontal and then in the vertical direction), measuring the distances between the ruled markings as they appeared on the television monitor, and comparing these distances with the actual ruler spacings. Measurements were made for the 1-cm ruled markings with the thumb wheel set for 1:1 magnification, and for the 0.5-cm ruled markings at 4.3:1 magnification. The 1:1 magnification was set by imaging a pair of markings, 1 cm apart, oriented horizontally at the center of the screen, and adjusting the thumb wheel control until the separation measured 1 cm on the monitor. Graphs of spatial distortion are shown in Fig 4.

Fig 2. A black-and-white transparency as it appears on the television monitor for several values of the local background, α, and local contrast, σ_D parameters of the image processing algorithm (the Wallis equation). (A) Bypass mode; (B) maximum background subtract, average contrast ($\alpha\uparrow$, σ_D); (C) minimum background subtract, average contrast ($\alpha\downarrow$, σ_D); (D) maximum contrast, average background subtract (α, $\sigma_D\uparrow$); (E) minimum contrast, average background subtract (α, $\sigma_D\downarrow$).

CONSPICUITY OF CALCIFICATIONS

To characterize the ability of the enhancer to assist in the identification of microcalcifications, a Nuclear Associates Mammographic QA phantom (model 76-001-4; Carle Place, NY) was used (Fig 5). The phantom consists of a 10-cm diameter, 3.7-cm thick acrylic block, which the manufacturer states is equivalent to an average breast compressed to a thickness of 4.5 cm. In addition to a set of nylon fibers that simulate soft tissue fibrils, the phantom contains five groups of simulated microcalcifications, composed of calcium carbonate, ranging from 0.12 to 0.35 mm in diameter. Each group contains three identical

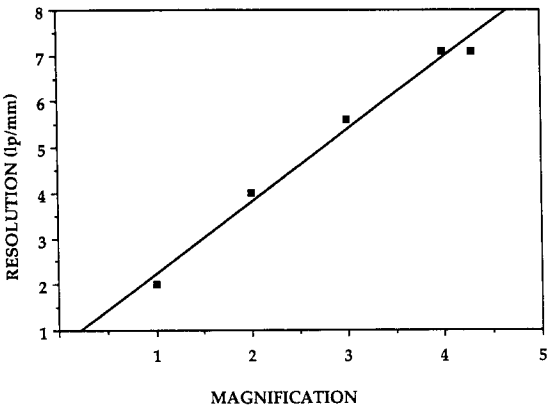

Fig 3. System resolution as a function of image magnification. High-contrast resolution.

calcifications arranged in a triangle. All the simulated calcifications lie in the same plane, which lies 3 cm from the bottom of the phantom.

Eleven contact radiographs of this phantom were made in our Thompson CGR Senographe 500t mammography unit (CGR, Inc, Baltimore, MD) to give a range of average optical densities (0.21 to 1.86 including base plus fog). A large focal spot size (0.44 mm × 0.39 mm as measured with a 2° Siemens star pattern) was used at 25 kV (peak) with a grid, and a focal-spot-to-film distance of 65 cm.

Four individuals, none of whom were radiologists, were given instructions on the operation of the image enhancer. They were shown a 2× magnified radiograph of the phantom and knew in advance both the locations and appearances of the calcifications. This allowed us to separate the problem of finding calcifications (which is highly dependent upon the skill of the mammographer)

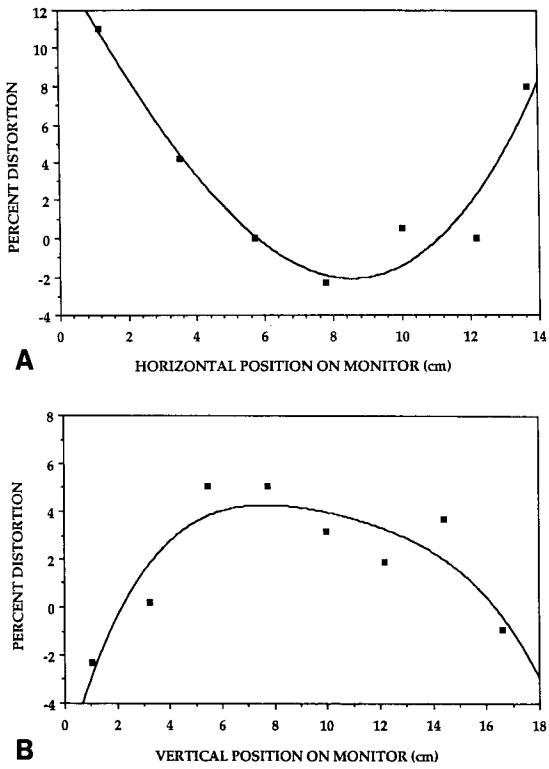

Fig 4. Percent spatial distortion as a function of position on the television monitor for 4.3:1 magnification: (A) left-to-right distortion; (B) top-to-bottom distortion.

from the ability of the image enhancer to increase their conspicuity. The radiographs were then viewed under three different conditions: (1) on a light box (with the unaided eye in a darkened room), (2) with the enhancer at maximum magnification on bypass mode, and (3) using the magnification, contrast, and background control features of the enhancer to opti-

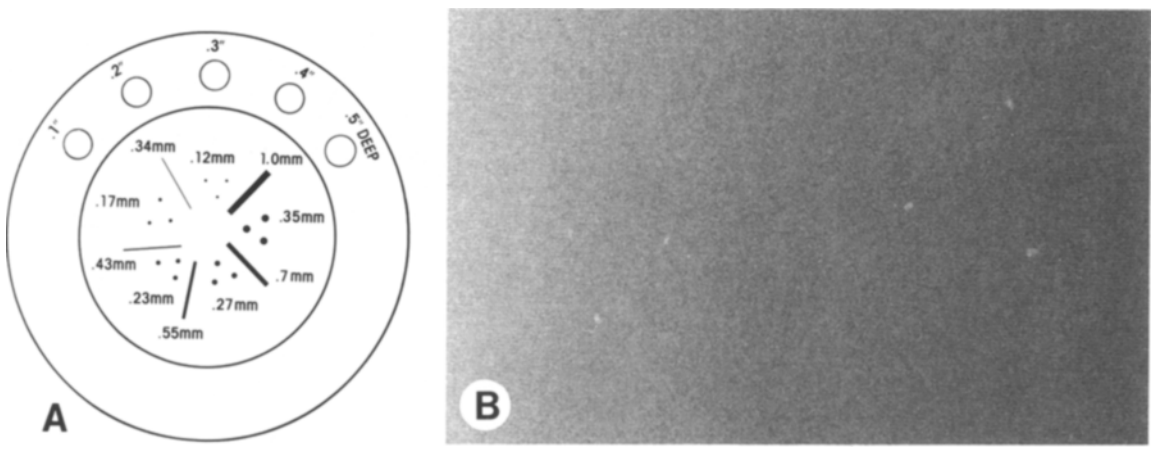

Fig 5. (A) Diagram of the Nuclear Associates Mammographic QA phantom. (B) Photograph of microcalcification groups 3 (0.23 mm) and 4 (0.17 mm) of a magnified radiograph (2×) of the phantom.

mize calcification conspicuity. Each investigator was asked to identify the number of the smallest diameter calcifications seen (with a high degree of confidence) in each radiograph. The experiment was then repeated by viewing the radiographs of the phantom with a slightly underexposed mammogram (average optical density, 0.31) overlaid on the film, thereby producing composite images ranging in density from 0.52 to 2.17 (Fig 6).

All the above experiments were carried out twice by three of the four investigators to ascertain what effect repetition of the same task had on the observer's ability to detect calcifications.

DATA ANALYSIS

Observations were quantified by assigning a number, S, called the conspicuity score, to each film and viewing condition according to the formula,

$$S = N_G + (N_C - 1)/3 \quad \text{(Equation 3)}$$

where N_G is the group number of the smallest calcifications(s) seen and N_C is the number of calcifications observed in that group. Groups are numbered from one to five in order of decreasing calcification diameter. Thus the conspicuity score, as defined by Equation 3, is a convenient method for recording the number of calcifications observed within a given group. For example, a conspicuity score of 2.67 represents the fact that three calcifications ($N_c = 3$) from group 2 (0.27 mm diameter) were observed.

For each radiograph viewed and for each investigator, the differences in conspicuity scores were calculated for three different pairs of viewing conditions. Pairing the data for each observer allowed us to test the image-enhancement system in a manner that minimizes the variations in ability among individuals in recognizing calcifications. The overall average of these differences (for all observers and all optical densities) was used to give a general characterization of the enhancement qualities of the system for different pairs of viewing conditions.

Table 1 shows the average differences (averaged over all observers and the 11 radiographs) in the number of additional calcifications de-

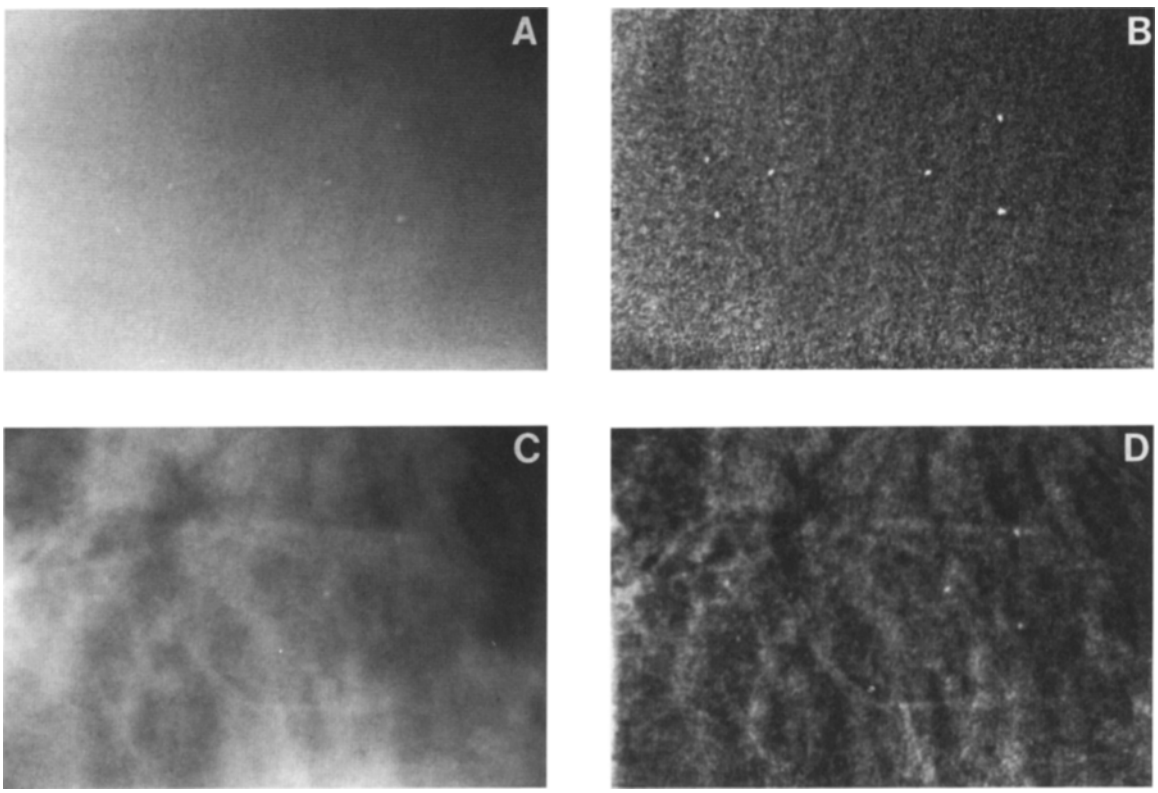

Fig 6. Photographs of groups 3 and 4 of a contact radiograph of the phantom as it appears on the television monitor at 4.3:1 magnification. Enhancer controls are set at (A) bypass mode and (B) maximum contrast, average background. (C) and (D) are the same as (A) and (B), except the radiograph of the phantom is overlaid with a mammogram.

Table 1. Increase in the Average Number of Calcifications Detected per radiograph (N) for Three Pairs of Viewing Conditions: Image Enhancement (all features), Bypass Mode (magnification only), and Light Box (unaided eye)

Viewing Conditions	N	*P* Value
Phantom alone		
Enhancer/lightbox	1.43	$<10^{-6}$
Bypass/lightbox	0.44	$<10^{-4}$
Enhancer/bypass	0.99	$<10^{-5}$
Phantom plus mammogram		
Enhancer/lightbox	1.08	$<10^{-5}$
Bypass/lightbox	0.07	0.40
Enhancer/bypass	1.01	$<10^{-5}$

NOTE. *P* values were calculated using a single-tailed paired-data *t* test.

tected per radiograph for three pairs of viewing conditions. These numbers were calculated by taking the average difference in conspicuity scores for each pair of viewing conditions and multiplying by three. Table 2 is a tabulation of the data as a function of the average optical density of the radiographs. Figure 7 shows graphs of absolute conspicuity scores (Equation 3) as a function of optical density for the phantom images alone and for the phantom images with mammogram overlay.

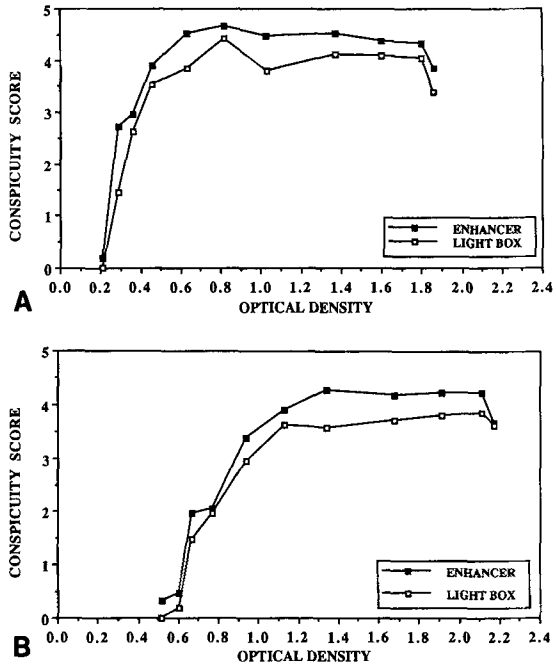

Fig 7. Average absolute conspicuity scores as a function of optical density: (A) phantom only; (B) phantom with overlaid mammogram.

DISCUSSION

The high-contrast resolution measurements of 2 lp/mm (magnification, 1:1) and 7.1 lp/mm (magnification, 4.3:1) correspond to resolving power distances of 250 μm and 70 μm, respectively. Calculations based on measurement of the high-contrast resolution in the horizontal direction (perpendicular to the television monitor lines) showed the monitor to have a band-pass frequency of 5.8 MHz. This is slightly above average. Typical television monitors provide equal resolution in both the horizontal and vertical directions, whereas this monitor gave an above-average resolution in the horizontal direction.

Spatial distortion at maximum magnification is less than 10%, providing one is at least 0.5 cm away from the extreme edges of the screen (Fig 4). This can be partially corrected by adjusting the linearity controls on the monitor and ensuring that the optical system is properly aligned.

Regarding conspicuity, the results in Table 1 show that using the enhancer (with all the

Table 2. Increase in the Average Number of Calcifications Detected per Radiograph (N) as a Function of Film Density

Phantom Only			Phantom Plus Mammogram		
OD	N Enhancer/Lightbox	*P* Value	Optical Density	N Enhancer/Lightbox	*P* Value
0.21	0.57	0.18	0.52	1.00	0.09
0.29	3.86	0.009	0.60	0.86	0.13
0.36	1.00	0.04	0.67	1.43	0.08
0.46	1.14	0.02	0.77	0.29	0.08
0.63	2.00	0.001	0.94	1.28	0.02
0.82	0.71	0.07	1.13	0.86	0.04
1.03	2.00	0.002	1.34	2.14	0.001
1.37	1.28	0.009	1.68	1.43	0.04
1.60	0.86	0.007	1.91	1.29	0.12
1.80	0.86	0.02	2.11	1.14	0.06
1.86	1.43	0.02	2.17	0.14	0.41

NOTE. *P* values were calculated using a single-tailed paired-data *t* test.

features) resulted in average observed increases of 1.4 and 1.1 microcalcifications detected (per radiograph) for the phantom alone and phantom plus mammogram overlay, respectively. If the increase of 3.86 microcalcifications at 0.29 optical density in Table 2 is considered an outlier, then the average of 1.4 reduces to 1.2, which is statistically indistinguishable from 1.1. However, it should be emphasized that of the additional simulated microcalcifications detected using the full features of the enhancer, 69% and 78% were from the next smaller group for the phantom and phantom plus mammogram, respectively. These increases are relative to using a lightbox with the unaided eye.

The bypass mode at maximum magnification (4.3:1) led to average respective increases of only 0.44 and 0.07 additional microcalcifications (per radiograph) being detected. Because the P values for increased conspicuity were typically $< 10^{-5}$, indicating a high level of statistical significance, it is clearly the imaging processing algorithm controlling image contrast and background level that is primarily responsible for the improvements in microcalcification detection. Magnification alone accounts for only a small fraction of the conspicuity increases.

For the series of experiments carried out in this report, the IMAGE REVERSAL, EDGE ENHANCEMENT, CIRCULAR REGION OF INTEREST, and SPLIT-SCREEN features were of limited value.

Repeating all the observations a second time (within 2 weeks of the initial observations) resulted in relatively small increases in conspicuity scores, with one major exception. For the phantom radiographs with the mammogram overlay, the average number of additional calcifications detected (per radiograph) increased from 0.80 to 1.45 when the full features of the enhancer were used compared with using only the light box.

CONCLUSION

As implemented by the Damon image-enhancement system, the video processing algorithm based on the Wallis equation gives statistically significant increases in microcalcification conspicuity for radiographs of the Nuclear Associates Mammographic phantom, as well as radiographs of this phantom overlaid with a mammogram. These increases were caused primarily by the contrast and background control features of the image processor and not to magnification. A quantitative evaluation of the enhancer's performance in a clinical setting cannot be predicted from the results presented here. One major reason is that the positions and existence of microcalcifications will no longer be known a priori; thus, the effectiveness of the image enhancer becomes dependent on the experience and ability of the mammographer. However, qualitatively, we believe our results to be indicative of what can be expected clinically, although further investigation is necessary.

REFERENCES

1. Nguyen MT, Sickles EA: Radiographic detectability of breast microcalcifications: In vitro studies using a wide range of mammography techniques. Society of Photo-Optical Instrumentation Engineers Applications of Optical Instruments in Medicine, vol 173. Washington, DC, 1979, pp 129-134

2. Haus A, Dodd G, Paulus D: Historical review of mammographic imaging techniques in terms of image quality and reduced radiation dose. Society of Photo-Optical Instrumentation Engineers Applications of Optical Instruments in Medicine, vol 173. Washington, DC, 1979, pp 120-128

3. Andrews HC: Monochrome digital image enhancement. Appl Optics 15:495-503, 1976

4. Schreiber WF: Image processing for quality improvement. Proc Institute of Electrical and Electronic Engineers 66:1640-1651, 1978

5. Frost MM, Fisher HD, Nudelman S: A digital video acquisition system for extraction of subvisual information in diagnostic medical imaging. Proc Society of Photo-Optical Instrumentation Engineers 127:208-215, 1979

6. Ishida M, Kato H, Doi K, et al: Development of a new digital radiographic image processing system. Society of Photo-Optical Instrumentation Engineers Applications of Optical Instruments in Medicine, vol 347. 1982, pp 42-48

7. Driscoll EC Jr, Walker C: Local adaptive enhancement: a general discussion and fast implementation. Machine Processing of Remotely Sensed Data Symposium, 1983, pp 266-271

8. Wallis RH: An approach to space variant restoration and enhancement of images. Proc Symp Current Math Prob Image Science, Naval Postgraduate School, Monterey, CA, November 1976

9. Hier RG, Smith GW: Real-time local adaptive video processing in diagnostic imaging. Proc SPIE 535:298-301, 1985